

# Intratumoral Distribution of Tritiated-FDG in Breast Carcinoma: Correlation between Glut-1 Expression and FDG Uptake

Raya S. Brown, Jennifer Y. Leung, Susan J. Fisher, Kirk A. Frey, Stephen P. Ethier and Richard L. Wahl  
Division of Nuclear Medicine, Department of Internal Medicine, and Departments of Neurology and the Mental Health Research Institute, Radiation Oncology and Radiology, University of Michigan Medical Center, Ann Arbor, Michigan

Increased expression of glucose transporters is frequently associated with transformation and is often found in malignant tumors. To assess the relationship between cellular glucose transporter Glut-1 (brain/erythrocyte) and FDG uptake in malignant tumors we studied the expression of Glut-1 and  $^3\text{H}$ -FDG uptake in a syngeneic rat mammary cancer (RMC), an animal tumor model that closely mimics human breast carcinoma. **Methods:** Tumors of 1–9 RMT cell line were grown in female Lewis rats and were studied by immunoperoxidase staining with anti-Glut-1 antibodies, macro- and microautoradiography and densitometry following intravenous injection of  $^3\text{H}$ -FDG. **Results:** Most of the cancer cells contained Glut-1 positive cytoplasmic granules. Cells with strongly stained cell membrane were mainly observed in areas of intensive intraductal proliferation and high tumor cell density. No staining was observed in necrotic areas, connective tissue stroma or granulation tissue. FDG uptake in areas of high cancer cell density was consistently higher than average tumor uptake. Silver grain counts were  $31 \pm 8/0.023 \text{ mm}^2$  in regions of viable cancer cells, and were higher as compared to  $10 \pm 7$  counted in necrotic or  $8 \pm 8$  in connective tissue areas ( $p = 0.0001$ ). Densitometry of the autoradiograms and of the histochemically stained consecutive sections showed positive correlation between estimates of FDG uptake and the intensity of staining of the Glut-1 antigen ( $r = 0.3\text{--}0.6$ ;  $p = 0.0001$ ). **Conclusion:** Our results demonstrate significant positive correlation between the expression of the facilitative glucose transporter Glut-1 and FDG accumulation in viable cancer cells in the syngeneic rat breast cancer. They suggest that the regulation of FDG uptake may be mediated by Glut-1 and the heterogeneous expression of Glut-1 and tracer uptake may reflect localized variations in the metabolic conditions.

**Key Words:** breast carcinoma; Glut-1 expression; autoradiography; FDG uptake

**J Nucl Med 1996; 37:1042–1047**

Accelerated rates of glucose uptake and metabolism are frequent characteristics of transformed and malignant cells as well as experimental and human solid tumors (1–3). The malignancy-linked increase in glucose uptake is associated with an increase in hexose transport across the cell membrane (3,4), increased expression of glucose transporters (5–10) and changes in the levels and/or activity of glycolytic enzymes, specifically hexokinase and glucose-6-phosphatase, as compared to normal tissues (11–13). When glucose analogs such as 2-fluoro-2-deoxy-D-glucose (FDG) are administered in vivo, the net result of these changes is a preferential accumulation and metabolic trapping of FDG-6-phosphate in malignant tumors (14). This higher-than-background tumor accumulation

of FDG-6-phosphate is applied clinically when imaging tumors by  $^{18}\text{F}$ -FDG-PET.

Increased expression of histochemically detectable glucose transporter-1 (Glut-1) as compared to surrounding normal tissue has been recently reported in human breast cancer (7) and in the clear/acidophilic cell tumors in rat kidneys (15). In addition, above-tumor-average expression of Glut-1, mostly membranous, in tumor cell layers surrounding necrotic foci was observed in some of these tumors (7,8). Higher-than-tumor-average grain densities in areas surrounding small necrotic foci were also seen in microautoradiograms of human adenocarcinoma xenografts (HTB77 IP3) after intravenous injection of tritiated FDG (16). We hypothesized that cells in the vicinity of necrotic areas, which are likely to be subjected to hypoxic conditions, may adapt to an increased dependency on glycolysis as their main energy source by enhancing hexose transport and utilization. Indeed, an increase in FDG uptake and an increase in Glut-1 expression were found in HTB77 IP3 cells when they were exposed in vitro to a low oxygen atmosphere (17).

To verify the hypothesis that enhanced FDG uptake is associated with increased expression of Glut-1 in solid tumors we (1) studied the pattern of the cellular localization and the intratumoral distribution of histochemically detectable Glut-1 (2). We also examined the relationships between FDG uptake and Glut-1 expression in a syngeneic rat mammary carcinoma (RMC), an animal tumor model that closely mimics human breast carcinoma (18). We recently reported that in this human breast cancer model, FDG accumulates primarily in viable cancer cells and that the contributions of macrophages and other nonmalignant components to the total uptake of the glucose analog in untreated tumors is small. The uptake of FDG by the malignant component of the tumor, however, is heterogeneous, with the highest levels recorded in areas of extensive intraductal proliferation and densely packed cancer cells and considerably less retention in either large or small foci of necrosis (19).

The results, that sites of relatively high FDG uptake coincide with sites of high membranous expression of Glut-1 glucose transporter, suggest a causal relationship between Glut-1 expression and FDG uptake in this tumor model. The connections between tumor morphology, heterogeneous expression of Glut-1 and FDG uptake are discussed in this article.

## MATERIALS AND METHODS

### Animals

Female Lewis rats were injected with  $1 \times 10^6$  cells of transplantable rat mammary tumor cell line 1–9 RMT (18) into the interscapular fat pad. When the size of the tumors reached about 1–2 cm in diameter (about 6 wk postinoculation), animals were fasted overnight, five of them were injected intravenously with 100  $\mu\text{Ci}$  of deoxy-2-fluoro-D-glucose 2 ( $^3\text{H}$ ) ( $^3\text{H}$ -FDG) in 0.2 ml saline and one animal was injected with 0.2 ml saline (control

Received Mar. 31, 1995; revision accepted Aug. 21, 1995.

For correspondence or reprints contact: Richard L. Wahl, MD, Division of Nuclear Medicine, University of Michigan Medical Center, 1500 E. Medical Center Dr., B1G 412, Ann Arbor, MI 48109-0028.

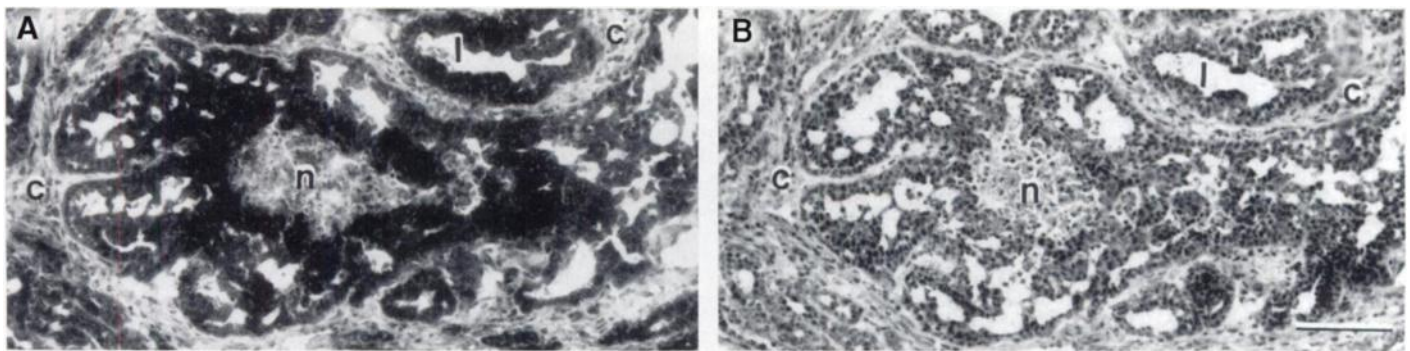


**FIGURE 1.** Glut-1 expression in RMC tumor grown on syngeneic rat. Micrographs of a duct from RMC tumor (tumor 2). (A) Section immunostained with anti-Glut-1 antibody. Most of the cancer cells are Glut-1 positive. The intensity of staining is heterogeneous and is lowest in cancer cells situated near the circumference of the duct. (B) Sequential section stained with anti-Glut-1 pre-mixed with the Glut-1 antigen (control). No immunostaining was observed. l = lumen; n = necrosis and inflammatory infiltrate; c = connective tissue stroma surrounding a duct. Magnification = 120 $\times$ ; Bar = 100  $\mu$ m.

animal for the autoradiography to rule out chemography). The tumors were removed 2 hr postinjection to ensure high tumor-to-background ratios (20). Each of the tumors (n = 6) were divided into two parts: one part was frozen in iso-pentane (2-methylbutane) cooled in liquid nitrogen and stored at  $-70^{\circ}\text{C}$ ; the second part was fixed overnight in buffered formalin at  $4^{\circ}\text{C}$  and embedded in paraffin. Two additional tumors were fixed in Karnovsky fixative (21) and embedded in glycolmethacrylate to be used for microautoradiography (16).

#### Antibodies

Polyclonal rabbit anti-glucose transporter antibody reactive with Glut-1 (brain/erythrocyte transporter) was used to evaluate Glut-1 expression in the tumors. The antibody was raised in rabbit against synthetic peptides (13-mer) based on the deduced amino acid sequence of the carboxy terminus of the rat brain glucose transporter (CGLFHPLGADSQV) (22). It immunoreacts with an approximately 50,000 Da. glucose transporter species in rat brain and human erythrocytes and cross-reacts with the glucose transporter of human hepatocarcinoma cells (HEP G2) (23).

#### Immunohistochemistry

The expression of Glut-1 was studied in formalin-fixed frozen (6  $\mu$  thick) and paraffin (3  $\mu$  thick) sections of the RMC tumors. The sections were incubated with anti-Glut-1, and the bound antibody was visualized by the avidin/biotin conjugate immunoperoxidase procedure (ABC) (24) using the Vectastain Elite kit (Vector, Burlingame, CA) (7). Consecutive sections incubated with normal rabbit IgG or with a mixture of the anti-Glut-1 with excess of the C-terminus peptide antigen were used as negative controls. Sections from paraffin-embedded brain, liver and kidney from normal fasted rat were used as positive controls.

#### Autoradiography

**Microautoradiography.** Dried frozen sections (6  $\mu$  thick) and sections (3  $\mu$  thick) from glycolmethacrylate (GMA)-embedded tumors were autoradiographed in order to directly verify the localization of the FDG in the macroautoradiograms. Although dipping frozen sections causes diffusion and GMA-embedding results in considerable loss of radioactivity and diffusion, it has been our experience that intratumoral localization and density distribution of the silver grains in such autoradiograms is qualitatively similar to that obtained in macroautoradiograms of dried frozen sections. Moreover, the emulsion layer on the glycolmethacrylate sections is smooth and more uniform resulting in autoradiograms with better efficiency and resolution and extremely good morphological quality, while the emulsion layer formed on frozen sections tends to be irregular due to their uneven surface (25). Additionally, their morphological quality is inferior. It was therefore assumed that the silver grain localization and density distri-

bution in these autoradiograms may provide strong supportive data to the results obtained from the macroautoradiograms. Sections from the two GMA-embedded tumors and dried frozen sections from the other six tumors were dipped in NTB 2 nuclear emulsion diluted 1:1 in deionized distilled water and exposed at  $4^{\circ}\text{C}$  for 6 wk as was previously described (16). Grains were counted in areas of densely packed tumor cells, necrotic foci, granulation and connective tissue or lumens of ducts. Five  $63\times$  fields of same-size areas (grid area,  $150 \times 150 \mu\text{m}$ ) of each category in 11 sections of the 2 GMA-embedded tumors were counted.

**Macroautoradiography.** Sets of three consecutive frozen sections, sectioned at intervals of 800  $\mu\text{m}$  through the frozen part of the tumor, were collected on frozen slides ( $-20^{\circ}\text{C}$ ) and quickly dried on a hot plate to minimize diffusion. The dried sections and a set of calibrated plastic radioactive standards (26) were placed in x-ray cassettes and were apposed to hyperfilm- $^{3}\text{H}$  at room temperature for 29 days and were developed as was previously described (19).

#### Densitometry

Differences in relative FDG uptake were estimated from the variations in the relative optical densities of the autoradiographic film images by computer-assisted video densitometry (19,26). The densities along three transept lines (enclosed elongated areas that were five pixels high across the section) traversing computerized images obtained from each of two tumors were superimposed onto the coregistered computerized images of subsequent sections immunostained with anti-Glut-1 and the patterns of FDG levels and staining intensities were compared.

Glut-1 staining intensities were estimated based on an arbitrary gray scale (between background outside the section and area of the maximum intensity on the section). FDG uptake was estimated by a set of standards (19). Correlations between FDG uptake and Glut-1 expression were calculated from these data.

## RESULTS

#### Histology

The tumors displayed morphology of intraductal carcinomas (19). Generally, the glandular parenchyma contained areas of extensive intraductal proliferation that often formed foci consisting solely of clustered cancer cells. These foci were often situated at the center of a large duct and measured about  $150 \times 100 \mu\text{m}^2$  and contained 4–5 rows of cancer cells. Other areas contained clusters of differentiated ducts of various sizes. These ducts were lined in most cases with a monolayer of cancer cells (Figs. 1–3). Most of the necrotic foci in these tumors were microscopical in size, they were usually confined to ductal lumens in a comedocarcinoma-like pattern and often infiltrated by inflammatory cells. The connective tissue stroma supporting the

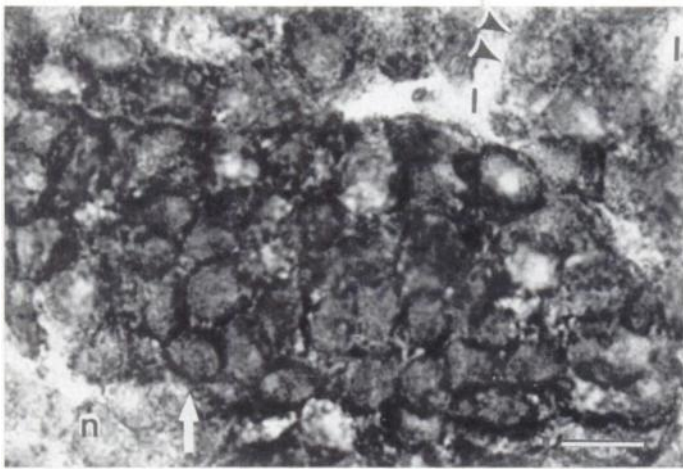


**FIGURE 2.** Glut-1 expression in RMC tumor grown on syngeneic rat. Micrograph of frozen section (tumor 2) of Glut-1 positive cancer cells. The highest intensity of staining is observed along the cell membrane of densely packed cancer cell inside the lumen (white arrows) of a duct. Glut-1 positive granules are seen in the cytoplasm of cancer cells forming a monolayer along the circumference of the same duct (arrowheads). Note that the cell membranes of these cancer cells are not intensely stained. Mag = 1000 $\times$ ; Bar = 10  $\mu$ m.

cancer cells was thin and little granulation tissue was seen around the tumor. Arterioles and venules could be identified in the connective tissue stroma encircling the ducts only.

#### Immunohistochemistry

Glut-1 positive cells were observed in both frozen and paraffin sections and the intensity of staining was heterogeneous. In frozen sections, Glut-1 positive cytoplasmic granules were observed in most of the cancer cells (Fig. 1). In these sections, the lowest intensity of staining was observed in cancer cells situated near the circumference of the duct. The highest intensity of staining was seen in cancer cells situated near the center of the ducts, bordering the area containing necrotizing cells and inflammatory infiltrate or away from the connective tissue stroma surrounding the ducts (Fig. 1A). In these areas, high expression of Glut-1 was observed in the cell membranes in addition to the cytoplasmic granules (Fig. 1A, Fig. 2). In paraffin sections, the staining was more localized than that observed in the frozen sections and was seen most frequently in the membrane of clustered cancer cells and cancer cell layers near necrotic foci (Fig. 3).

Staining of Glut-1 positive controls was in agreement with published data: There was staining of endothelial cells lining the blood vessels in paraffin sections of rat brain (27), the

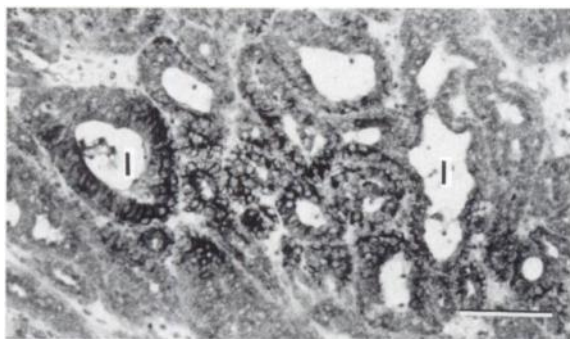


**FIGURE 3.** Glut-1 expression in RMC tumor grown on syngeneic rat. Micrograph of paraffin section (tumor 1) that was incubated with anti-Glut-1. Note that mostly membranes of cells organized in multi layers are Glut-1 positive. It appears that dehydration and embedding in paraffin resulted in the loss in Glut-1 immunogenicity of the cytoplasmic granules. Mag = 120 $\times$ ; Bar = 100  $\mu$ m.

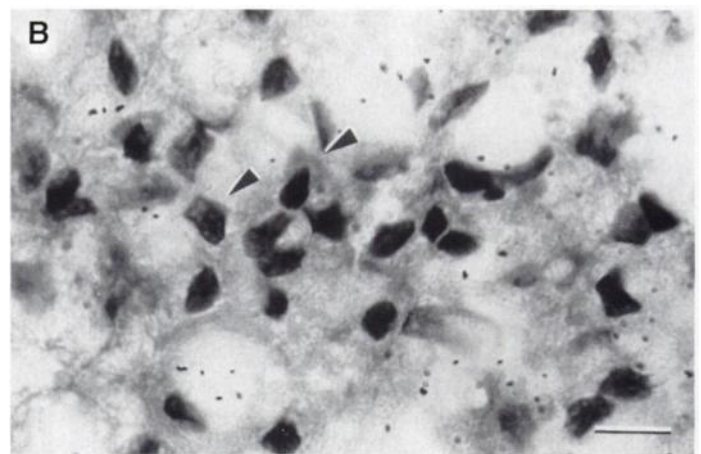
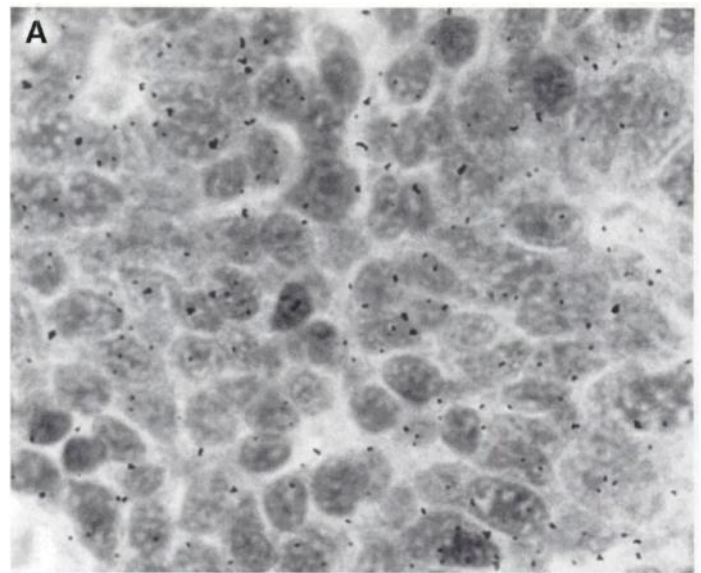


**FIGURE 4.** Distribution of silver grains in dried frozen section in RMC tumor grown on syngeneic rat (tumor 6). Sections were dipped in NTB2 emulsion. Mag = 800 $\times$ ; Bar = 10  $\mu$ m. (A) An area of densely packed cancer cells. (B) An area of necrosis in the lumen of a duct. Note shrunken cells with angular cytoplasm and pyknotic nuclei (arrowheads).

epithelium of certain segments of the renal tubules both in the cortex and the medulla as well as the collecting ducts in the kidney (28). In hepatocytes faint granular staining was sometimes seen but there was no staining of the cells' membranes (29). Incubating with normal rabbit serum or with a mixture of antibody and excess of the carboxy-end peptide (antigen) completely abolished the staining in the paraffin-embedded tissues and the normal rat tissue controls. In frozen sections of the tumors that were stained with either the mixture or the non-immune rabbit serum, cancer cells were negative (Fig. 1B).

#### Autoradiography

**Microautoradiography.** More silver grains were observed in areas with extensive intraductal proliferation and clustered cancer cells than in the lumens, necrotic foci or connective tissue stroma in both GMA sections and dried frozen sections (Fig. 4). Similar distributions of radioactivity were observed in macroautoradiograms of subsequent dried frozen sections (19). The grain counts in areas solely consisting of cancer cells were 3-to-5 times higher than in ductal lumens, foci of necrosis/inflammatory-cell infiltration or connective/granulation tissues (Table 1). The differences between the grain counts in areas of cancer cells and any of the other histological categories were statistically significant ( $p = 0.0001$ ). No differences in grain

**TABLE 1**  
Number of Grains in the Different Morphological Areas of Syngeneic RMC  
(Grains/150 × 150 mm of section at 630x)\*

Tissue category	No. of grains (mean ± s.d.)
Granulation/Connective tissue	8.2 ± 7.7
Necrosis/Inflammatory infiltration	9.7 ± 6.5
Lumens	13.5 ± 8.9
Cancer cells	30.7 ± 8.0†

\*Five fields per category in each of eleven sections were counted.  
†The number of grains counted over this area was higher than the number of grains counted over any of the other area ( $p = 0.0001$ ).

counts over granulation/connective tissue, necrosis/inflammatory infiltration or the ductal lumens were found.

**Macroautoradiography.** The autoradiograms showed that the areas of high FDG accumulation corresponded to areas of the tumor proper. The activity present in the granulation tissue surrounding these syngeneic tumors or in visibly discernible necrotic areas was very low. Areas of high FDG uptake in the autoradiograms appeared to correlate with areas where high expression of Glut-1 was observed, namely foci consisting exclusively of cancer cells [Fig. 2, Fig. 5 and (19)]. Variations in the relative densities along the transept lines from the autoradiograms were significantly correlated with the variations in the staining intensity in the parallel areas in the sequential immunostained slide ( $r = 0.3-0.6$ ;  $p = 0.0001$ ) (Fig. 6).

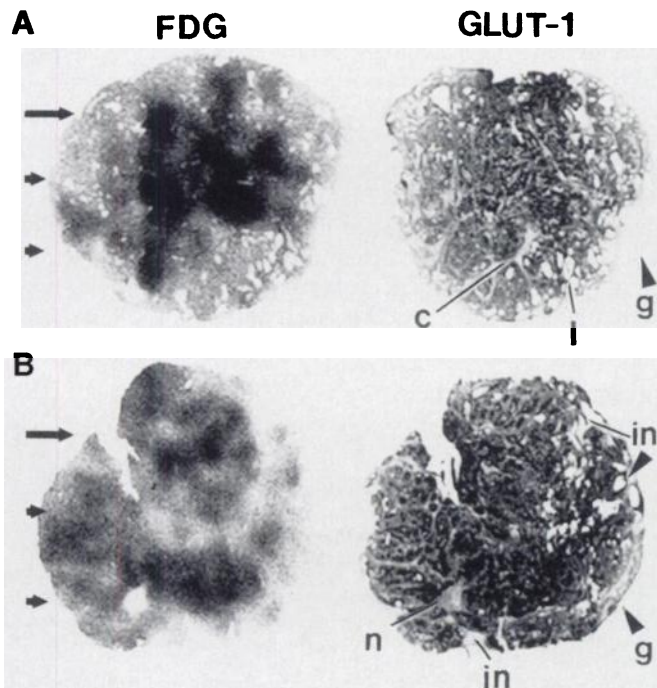


**FIGURE 5.** Glut-1 expression and FDG uptake in RMC tumors grown in syngeneic rat. (A) Computerized images of an autoradiogram (top left) and of a Glut-1 stained consecutive frozen section (top right) from tumor 4 (RMC 4). (B) Computerized image of an autoradiogram (bottom left) and of a Glut-1 stained consecutive frozen section (bottom right) from tumor 6 (RMC 6). The darkest areas (high FDG uptake) in the autoradiograms corresponded to regions of highest Glut-1 staining. c = connective tissue stroma; g = area of primarily granulation tissue; in = area of primarily infiltrating inflammatory cells; l = lumens of ducts; n = area of primarily necrotizing cancer cells. Necrotic areas usually contained many infiltrating inflammatory cells.

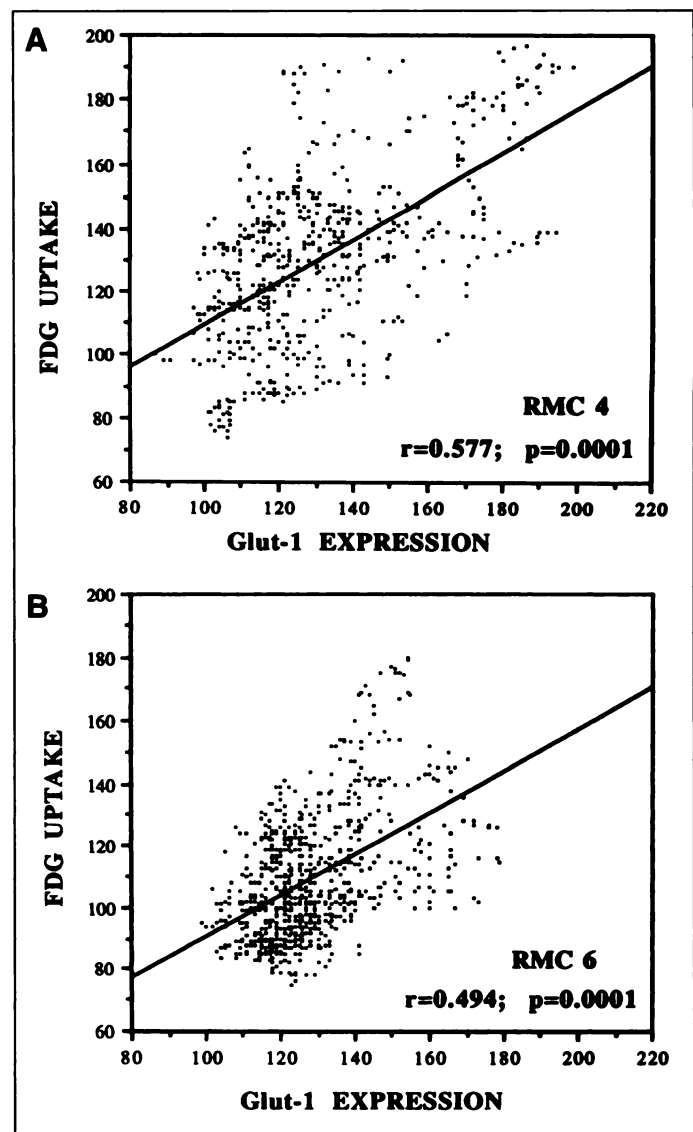


**FIGURE 6.** Correlation between FDG uptake and Glut-1 expression in RMC tumors grown on syngeneic rat. Relative optical densities were estimated by computer-assisted video densitometry. The number of pairs of data points was 582 for tumor 4 (RMC 4) and 851 for tumor 6 (RMC 6).

## DISCUSSION

In the syngeneic rat mammary cancer, sites of high FDG uptake, as estimated from both macro- and microautoradiograms, coincided with sites of high expression of the Glut-1. In these sites, which consisted primarily of viable cancer cells as judged by their morphology, immunostaining with anti-Glut-1 antibody showed distinctive high binding to the cell membranes in addition to cytoplasmic granules as seen in most of the cancer cells in these tumors. Analysis of the computerized images of macroautoradiograms and immunostained consecutive sections by semiquantitative scanning-densitometry revealed highly significant correlation between FDG uptake and Glut-1 expression. The association between FDG uptake and Glut-1 expression suggests a functional relationship between these two phenomena that are often linked to transformation and malignancy.

Increased rates of uptake of glucose and of glucose analogs, namely 2-deoxyglucose and FDG, as well as overexpression of facilitative glucose transporters have been reported in both human and animal cancers. An increased abundance of transporter in the cell membrane as a response to increased demands for glucose is considered to be a possible mechanism for

enhancing glucose influx into cells (30,31), and transmembrane transport mediated by specific transporters has been shown to be an important determinant in the regulation of the uptake of both glucose and FDG in tumor cells (4,32). The extensive binding of the anti-Glut-1 to the cell membrane of cancer cells in areas of high FDG uptake seen in RMC suggests that Glut-1 may be active in the transport of glucose into these cancer cells. Moreover, since the antibody was raised against the carboxy terminus of the transporter, which is the moiety of the transporter molecule that is active in the transport (33), the staining may also imply that the transporter molecules in these cells have the capability to mediate the transfer.

It is still not known to what extent FDG uptake depends on Glut-1 expression. For example, an increase of 150% of glucose uptake was associated with a 50% increase in membranous Glut-1 expression in cell membranes of the heart muscle exposed to anoxia (34) and the degree of transporter-mRNA induction by growth factor in mouse fibroblasts was never matched by the degree of transport or transporter-protein induction (35). Furthermore, in addition to transport across the cell membrane, intratumoral variation in blood flow (36) and the rates of intracellular phosphorylation and dephosphorylation (14) may have significant roles in the regulation of glucose influx and can affect the level FDG retained in cancer cells. Indeed it was found in untreated human primary breast cancers that regions with high blood flow generally have higher FDG uptake than regions with low flow (37). Nevertheless, the highly significant correlation between FDG uptake and Glut-1 expression does suggest that the transporter may contribute to the enhanced influx into cancer cells, although transport is not necessarily the sole or the rate-limiting step in the regulation of FDG uptake. The significance of Glut-1 mediated transport of sugars into breast cancer cells may be further supported by findings in the intact lactating mammary gland. It has been reported that in this gland transport is a rate-limiting factor in the utilization of carbohydrates (38); Glut-1 is overexpressed and only this transporter is present (39–41). Overexpression of Glut-1 in the cell membranes seen in cells in areas of high FDG uptake may serve as an additional indication of the causal relationship between the two phenomena.

The question is whether the intratumoral heterogeneity in transporter expression results from the diverse phenotypic properties of tumor cells or is induced by their metabolic microenvironment. The finding that the highest levels of Glut-1 expression are observed in clusters of viable cancer cells situated near the center of the ducts or in cell layers bordering sites of necrosis, sites that are likely to be subjected to less than ideal blood supply, may suggest dependency between the transporter expression, FDG uptake and the metabolic conditions. Such dependency has been reported in the heart muscle where ischemia induced increased FDG uptake (42,43), triggered translocation (34) and increased expression of Glut-1 (43). Similarly, high levels of radiolabeled FDG in cancer cells surrounding small necrotic foci, where they are likely to be exposed to some degree of ischemia and/or hypoxia, have also been reported in HTB77 IP3 xenografts in nude mice (16) and in syngeneic mouse mammary tumors following iv tracer injection (44). Moreover, a 50% increase in FDG uptake as well as a 10% increase in the number of cells expressing immunohistochemically detectable Glut-1 were found in cultured HTB77 IP3 cells exposed to low oxygen atmosphere (17) and relatively high transporter expression in the vicinity of neoplastic lesions was described in the rat kidney (8). The colocalization of high FDG levels and Glut-1 overexpression in areas that are likely to be subjected to hypoxia and the strong

correlation between the transporter expression and FDG uptake suggest that enhanced transmembrane transport may be a part of an adaptive mechanism triggered by changes in the metabolic microenvironment of cancer cells. The increased staining-intensity of cell membranes seen in sites of high FDG uptake may imply that the glucose-influx is regulated by translocation of transporter from cytoplasmic sites to the cell membrane.

Intracellular retention of FDG in cancer cells results from its phosphorylation by hexokinase (14,38,45) which depends on availability of ATP (46) and the inability of FDG-6-phosphate to diffuse out through the cell membrane. Therefore, it seems unlikely that FDG preferentially accumulates in necrotic cells with damaged membranes as has been suggested by Kubota et al. (44). Rather, it is feasible that FDG accumulates in viable cells that may have adapted to less-than-ideal microenvironmental conditions by translocation of transporter to the cell membrane and thus increase their glucose uptake by means of the transporter-mediated passive processes of facilitated diffusion not unlike the ischemic heart muscle (47,48). Furthermore, it has been suggested that an increased glucose uptake reflects continued cell viability (49) and it has been found that sites of high FDG uptake coincide with sites of 'new fill-in' of  $^{201}\text{Tl}$  (50) and  $^3\text{H}$ -uridine uptake (51), both indicators of cell viability in the ischemic myocardium. Adaptation to dependency on glucose as the energy source in microenvironment created in foci consisting exclusively of clustered cancer cells or in the vicinity of necrosis by an increased expression of glucose transporter can maintain cell viability and promote higher-than-tumor-average FDG accumulation.

## CONCLUSION

The presence of sites of co-localization of Glut-1 overexpression and higher-than-tumor-average FDG accumulation and the strong correlation between transporter expression and sugar uptake in this syngeneic breast cancer suggest that (1) a causal relationship may exist between these parameters implying that the rate of transmembrane influx of FDG is regulated by Glut-1 and (2) that heterogeneous expression of Glut-1 may reflect localized variations in tumor metabolism. Further studies are needed to determine whether the variations in FDG uptake are indicative of sites subjected to hypoxic conditions in tumors. Studies are also needed to determine whether increased expression of glucose transporters enable malignant cells to survive in an environment with a less than ideal milieu as is often present in fast growing tumors.

## ACKNOWLEDGMENT

Supported by National Cancer Institute grants CA 53172, CA 52880 and CA 56731.

## REFERENCES

1. Warburg O. *The metabolism of tumors*. New York: Richard R. Smith, Inc., 1931:29–169.
2. Watanabe A, Tanaka R, Takeda N, Washiyama K. DNA synthesis, blood flow and glucose utilization in experimental rat brain tumors. *J Neurosurg* 1989;70:86–91.
3. Flier JS, Mueckler MM, Usher P, Lodish HF. Elevated levels of glucose transport and transporter messenger RNA are induced by ras or src oncogenes. *Science* 1987;235:1492–1495.
4. Birnbaum MJ, Haspel HC, Rosen OM. Transformation of rat fibroblasts by FSV rapidly increases glucose transporter gene transcription. *Science* 1987;235:1495–1498.
5. Yamamoto T, Seino Y, Fukumoto H, et al. Overexpression of facilitative glucose transporter genes in human cancer. *Biochem Biophys Res Commun* 1990;170:223–230.
6. Su TS, Tsai TF, Chi CW, Han SH, Chou CK. Elevation of facilitated glucose-transporter messenger RNA in human hepatocellular carcinoma. *Hepatology* 1990;11:118–122.
7. Brown RS, Wahl RL. Overexpression of Glut-1 glucose transporter in human breast cancer: an immunohistochemical study. *Cancer* 1993;72:2979–2985.
8. Ahn YS, Zerban H, Bannasch P. Expression of glucose transporter isoforms (Glut-1, Glut-2) and activities of hexokinase, pyruvate kinase and malic enzyme in preneoplastic and neoplastic rat renal basophilic cell lesions. *Virchows Arch B Cell Pathol* 1993;63:351–357.

9. Nagamatsu S, Sawa H, Wakizaka A, Hoshino T. Expression of facilitative glucose transporter isoforms in human brain tumors. *J Neurochem* 1993;61:2048–2053.
10. Mellanen P, Minn H, Grenman R, Harkonen P. Expression of glucose transporters in head-and-neck tumors. *Int J Cancer* 1994;56:622–629.
11. Weber G. Enzymology of cancer cells (second of two parts). *N Engl J Med* 1977;296:541–551.
12. Som P, Atkins HL, Bandoypadhyay D, et al. A fluorinated glucose analog, 2-fluoro-2-deoxy-D-glucose (<sup>18</sup>F): nontoxic tracer for rapid tumor detection. *J Nucl Med* 1980;21:670–675.
13. Fischer G, Ruschenburg I, Eigenbrodt E, Katz N. Decrease in glucokinase and glucose-6-phosphatase and increase in hexokinase in putative preneoplastic lesions of rat liver. *J Cancer Res Clin Oncol* 1987;113:430–436.
14. Goldberg MA, Lee MJ, Fischman AJ, Mueller PR, Alpert NM, Thrall JH. Fluorodeoxyglucose PET of abdominal and pelvic neoplasms: potential role in oncologic imaging. *Radiographics* 1993;13:1047–1062.
15. Ahn YS, Zerbán H, Grobholz R, Bannasch P. Sequential changes in glycogen content, expression of glucose transporters and enzymic patterns during development of clear/acidophilic cell tumors in rat kidney. *Carcinogenesis* 1992;13:2329–2334.
16. Brown RS, Fisher SJ, Wahl RL. Autoradiographic evaluation of the intra-tumoral distribution of 2-deoxy-D-glucose and monoclonal antibodies in xenografts of human ovarian adenocarcinoma. *J Nucl Med* 1993;34:75–82.
17. Clavo A, Brown R, Lee R. 2-Fluoro-2-deoxy-D-glucose (FDG) uptake into human cancer cell lines is increased by Hypoxia. *J Nucl Med* 1995;36:1625–1632.
18. Ethier SP, Cundiff KC. Importance of extended growth potential and growth factor independence on in vivo neoplastic potential of primary rat mammary carcinoma cells. *Cancer Res* 1987;47:5316–5322.
19. Brown RS, Leung JY, Fisher SJ, Frey KA, Ethier SP, Wahl RL. Intratumoral distribution of tritiated fluorodeoxy-glucose in breast carcinoma: I. Are inflammatory cells important? *J Nucl Med* 1995;36:1854–1861.
20. Wahl RL, Hutchins GD, Buchsbaum DJ, Liebert M, Grossman HB, Fisher S. Fluorine-18-2-deoxy-2-fluoro-D-glucose uptake into human tumor xenografts. Feasibility studies for cancer imaging with positron-emission tomography. *Cancer* 1991; 67:1544–1550.
21. Karnovsky MJ. A formaldehyde-glutaraldehyde fixative of high osmolality for use in electron microscopy. *J Cell Biol* 1965;27:137A.
22. Birnbaum MJ, Haspel HC, Rosen OM. Cloning and characterization of a cDNA encoding the rat brain glucose-transporter protein. *Proc Natl Acad Sci USA* 1986;83: 5784–5788.
23. Haspel HC, Rosenfeld MG, Rosen OM. Characterization of antisera to a synthetic carboxyl-terminal peptide of the glucose transporter protein. *J Biol Chem* 1988;263: 398–403.
24. Hsu SM, Raine L, Fanger H. Use of avidin-biotin-peroxidase complex (ABC) in immunoperoxidase techniques: a comparison between ABC and unlabeled antibody (PAP) procedures. *J Histochem Cytochem* 1981;29:577–580.
25. Rogers AW. Techniques of autoradiography, 3rd ed. New York: Elsevier/North-Holland Biomedical Press; 1979:429.
26. Pan HS, Frey KA, Young AB, Penney J Jr. Changes in [<sup>3</sup>H]muscimol binding in substantia nigra, entopeduncular nucleus, globus pallidus and thalamus after striatal lesions as demonstrated by quantitative receptor autoradiography. *J Neurosci* 1983;3: 1189–1198.
27. Dermietzel R, Krause D, Kremer M, Wang C, Stevenson B. Pattern of glucose transporter (Glut-1) expression in embryonic brains is related to maturation of blood-brain barrier tightness. *Dev Dyn* 1992;193:152–163.
28. Dominguez JH, Camp K, Maiano L, Garvey WT. Glucose transporters of rat proximal tubule: differential expression and subcellular distribution. *Am J Physiol* 1992;262: F807–812.
29. Tal M, Schneider DL, Thorens B, Lodish HF. Restricted expression of the erythroid/brain glucose transporter isoform to perivenous hepatocytes in rats. Modulation by glucose. *J Clin Invest* 1990;86:986–992.
30. Ismail-Beigi F. Metabolic regulation of glucose transport. *J Membrane Biol* 1993;135: 1–10.
31. Merrill NW, Plevin R, Gould GW. Growth factors, mitogens, oncogens and the regulation of glucose transport. *Cell Signal* 1993;5:667–675.
32. Bramwell ME, Davies A, Baldwin SA. Heterogeneity of the glucose transporter in malignant and suppressed hybrid cells. *Exp Cell Res* 1990;188:97–104.
33. Tanti JF, Gautier N, Cormont M, Baron V, Van Obberghen E, Le Marchand-Brustel Y. Potential involvement of the carboxy-terminus of the Glut-1 transporter in glucose transport. *Endocrinology* 1992;131:2319–2324.
34. Wheeler TJ. Translocation of glucose transporters in response to anoxia in heart. *J Biol Chem* 1988;263:19447–19454.
35. Rollins BJ, Morrison ED, Usher P, Flier JS. Platelet-derived growth factor regulates glucose transporter expression. *J Biol Chem* 1988;263:16523–16526.
36. Vaupel P, Kallinowski F, Okunieff P. Blood flow, oxygen and nutrient supply and metabolic microenvironment of human tumors: a review. *Cancer Res* 1989;49:6449–6465.
37. Zasadny KR, Wahl RL. Regional FDG uptake versus blood flow in untreated primary breast cancers [Abstract]. *J Nucl Med* 1993;34(suppl):74P.
38. Threadgold LC, Kuhn NJ. Monosaccharide transport in the mammary gland of the intact lactating rat. *Biochem J* 1984;218:213–219.
39. Burnol AF, Leturque A, Loizeau M, Postic C, Girard J. Glucose transporter expression in rat mammary gland. *Biochem J* 1990;270:277–279.
40. Madon RJ, Martin S, Davies A, Fawcett HA, Flint DJ, Baldwin SA. Identification and characterization of glucose transport proteins in plasma membrane- and Golgi vesicle-enriched fractions prepared from lactating rat mammary gland. *Biochem J* 1990;272:99–105.
41. Camps M, Vilaro S, Testar X, Palacin M, Zorzano A. High and polarized expression of Glut-1 glucose transporters in epithelial cells from mammary gland: acute down-regulation of Glut-1 carriers by weaning. *Endocrinology* 1994;134:924–934.
42. Marshall RC, Tillisch JH, Phelps ME, Huang SC, Carson R, Henze E, Schelbert HR. Identification and differentiation of resting myocardial ischemia and infarction in man with positron computed tomography, <sup>18</sup>F-labeled fluorodeoxyglucose and <sup>13</sup>N-ammonia. *Circulation* 1983;67:766–778.
43. Brosius FCI, Sun D, England R, Nguyen N, Schwaiger M. Altered glucose transporter mRNA levels in cardiac ischemia. *Circulation* 1993;88:1–542.
44. Kubota R, Kubota K, Yamada S, Tada M, Ido T, Tamahashi N. Active and passive mechanisms of fluorine-18-fluorodeoxyglucose uptake by proliferating and preneoplastic cancer cells in vivo: a microautoradiographic study. *J Nucl Med* 1994;35:1067–1075.
45. Sokoloff L. Mapping of local cerebral functional activity by measurement of local cerebral glucose utilization with [<sup>14</sup>C]deoxyglucose. *Brain* 1979;102:653–668.
46. Reeves JP. Stimulation of 3-O-methylglucose transport by anaerobiosis in rat thymocytes. *J Biol Chem* 1975;250:9413–9420.
47. Kalff V, Schwaiger M, Nguyen N, McClanahan TB, Gallagher KP. The relationship between myocardial blood flow and glucose uptake in ischemic canine myocardium determined with fluorine-18-deoxyglucose. *J Nucl Med* 1992;33:1346–1353.
48. Opie LH, Camici PG. Myocardial blood flow, deoxyglucose uptake and myocyte viability in ischemia [Editorial]. *J Nucl Med* 1992;33:1353–1356.
49. Opie LH. Glycolytic rates control cell viability in ischemia. *J Appl Cardiol* 1988;3: 407–414.
50. Tamaki N, Ohtani H, Yonekura Y, et al. Viable myocardium identified by reinjection thallium-201 imaging: comparison with regional wall motion and metabolic activity on FDG-PET. *J Cardiol* 1992;22:283–293.
51. Yaoita H, Fischman AJ, Strauss HW, Saito T, Sato E, Maruyama Y. Uridine: a marker of myocardial viability after coronary occlusion and reperfusion. *Int J Cardiac Imaging* 1993;9:273–280.